

MB 2020-09

U-Pb geochronology report; Grenville 2019-2020

Documents complémentaires

Additional Files



Licence



License

Cette première page a été ajoutée
au document et ne fait pas partie du
rapport tel que soumis par les auteurs.

Énergie et Ressources
naturelles

Québec 



U-Pb geochronology report; Grenville 2019-2020

Konstantinos Papapavlou

MB 2020-09

Avertissement

Ce document est une copie fidèle du manuscrit soumis par l'auteur, sauf pour une vérification sommaire destinée à assurer une qualité convenable de diffusion.

U-Pb geochronology report;

Grenville 2019-2020

August 2020

Konstantinos Papapavlou, PhD

Post-doctoral research fellow

Volet Post-doctorant. (9 échantillons)

Par Konstantinos Papapavlou, PhD, Post-doctoral research fellow, GEOTOP-UQAM

SNRC	Fuseau	Estant	Nordant	No terrain	Unité (étiquette)	Type de roche	Âge de cristallisation (Ma)	Âge métamorphique (Ma)	Âge de déposition maximal (Ma)
32A16	18	717172	5427281	2019-AM-0092A1	Charnockite de Patrick Ouest (mPick1)	Granite à feldspath alcalin	1169 +/- 14		
32A15	18	646366	5427454	2019-AM-0002B1	Complexe de Barois (mPboi4c)	Quartzite			1237 +/- 8
32A15	18	660061	5423773	2019-FS-7085D1	Complexe de Barois (mPboi4c)	Quartzite			1224 +/- 18
32A15	18	665581	5412229	2019-AM-0167A1	Suite plutonique de Bardeau (mPbad)	Granite	1364 +/- 9	1090 +/- 41 Ma	
32A15	18	678010	5404499	2019-AM-0170A1	Suite plutonique de Saint-Méthode (mPstm)	Mangérite	1021 +/- 15		
32A15	18	656264	5414408	2019-AB-5002A1	Suite plutonique de Mimosa (mPmim1)	Mangérite	1015 +/- 13		
32A16	18	713961	5416418	2019-AM-0067A1	Mangérite de Lachance (mPlhc)	Mangérite	1031 +/- 17		
32A15	18	673599	5425086	2019-AM-0187A1	Barholite des Mailles (mPmas)	Mangérite	1039 +/- 15		
32A15	18	671843	5422401	2019-AM-0186A1	Suite de Saint-Thomas-Didyme (mPstd1)	Granite à feldspath alcalin	1042 +/- 12		

Tableau 1 : Récapitulatif des âges obtenus, avec incertitudes (2s)

1. Objectives

In this report are presented U-Pb isotopic, electron beam imaging, and optical microscopy data from samples that were collected in the Normandin area of the Lac-Saint-Jean region of Québec, during the period of July-August 2019. The U-Pb isotopic data were collected in GEOTOP-UQAM using Laser Ablation – High Resolution – Inductively Coupled Plasma – Mass Spectrometry (LA-HR-ICP-MS) whereas the electron beam imaging data using cathodoluminescence microscopy (SEM/CL). In this report are presented zircon U-Pb isotopic data from the samples 2019-AM-0092A1 (alkali feldspar-bearing granite), 2019-AM-0002B1 (quartzite), 2019-FS-7085D1 (quartzite), 2019-AM-0167A1 (granite), 2019-AM-0170A1 (mangerite), 2019-AB-5002A1 (mangerite), 2019-AM-0067A1 (mangerite), 2019-AM-0187A1 (mangerite), and 2019-AM-0186A1 (alkali feldspar-bearing granite). The zircon grains from the examined samples were separated following conventional gravitational and magnetic separation methods and were mounted in epoxy resin. The epoxy mounts (pucks) were polished until exposure of the interior part of grains and were imaged using cathodoluminescence microscopy before the LA-HR-ICP-MS isotopic analysis.

Sample 2019-AM-0092A1 (Alkali feldspar-bearing granite)

The examined zircon grains exhibit euhedral to subhedral faces with aspect ratios 2:1 up to 4:1 and commonly show more than two sets of fractures. In cathodoluminescence images the zircon grains show bright core domains that exhibit unzoned, homogeneous in CL signature or oscillatory zoning. Darker in CL domains with faint oscillatory zoning and/or convolute zoning are also observed. The

bright core domains are overgrown by different generations of darker mantle and rim domains of possible metamorphic origin (**Figure 1**). The U contents of the analysed grains vary from 42 to 783 ppm and the Th/U values from 0.15 to 0.61, the latter indicates igneous origin of the selected analytical domains. The analyses were conducted onto the core and mantle domains of grains with variable aspect ratios, external morphologies, and zoning types. In Wetherill-Concordia space the spot analyses yield an anchored to 0 ± 0 Ma upper intercept U-Pb date of 1169 ± 14 Ma (2σ , $n = 53$, MSWD = 0.56; Figure 2) that is interpreted as the crystallization age of the protolith and agrees within uncertainty with the age constraints of the first (1.16 – 1.13 Ga) AMCG-type magmatic pulse in the area of Lac-Saint-Jean (Higgins and Van Breemen., 1996). The analyses exhibit discordance values that vary from -3.3 to 15.3 % and possibly manifest variable degrees of Pb loss during later tectonothermal overprints. The upper intercept date of 1169 ± 14 Ma is slightly older than the U-Pb concordia age of the Charnockite of Patrick Ouest (1143.4 ± 2.4 Ma; Van Breemen, 2009) with the latter possibly being the rim of the Lac-Saint-Jean anorthositic Suite.

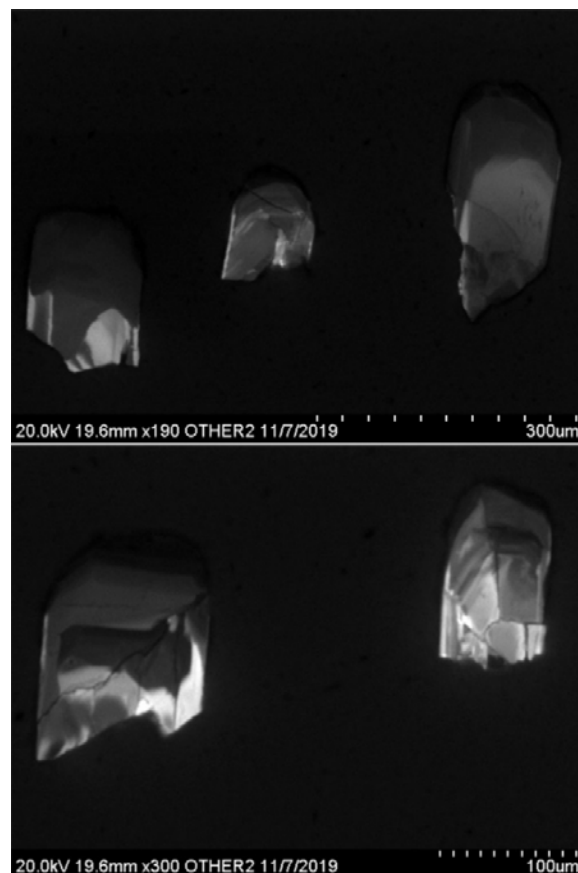


Figure 1. Representative cathodoluminescence images of zircon grains from the sample 2019-AM-0092A1

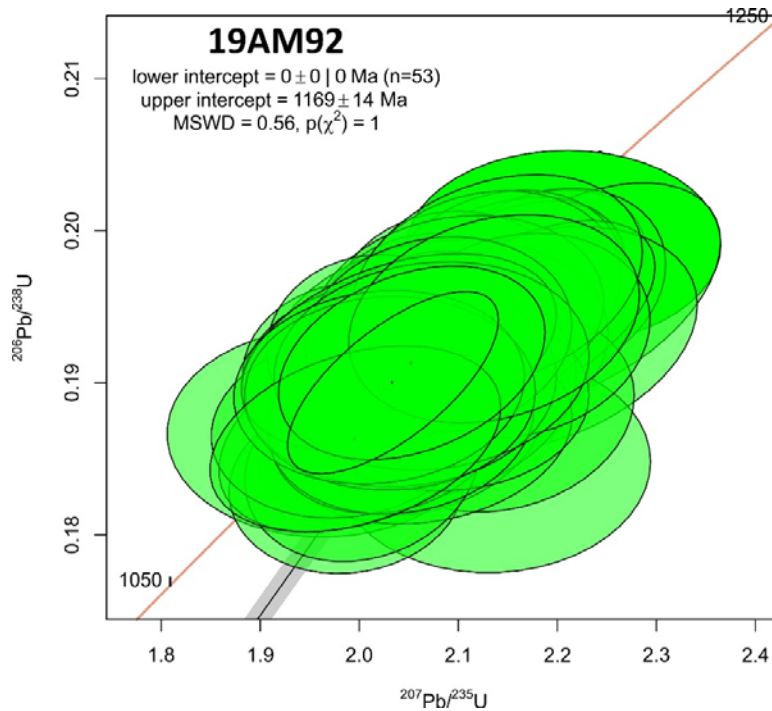


Figure 2. U-Pb concordia diagram with analyses of the sample 2019-AM-0092A1

Sample 2019-AM-0002B1 (Quartzite)

The zircon grains of the sample 2019-AM-0002B1 are rounded to subrounded with aspect ratios 1:1 to 2:1. The majority of the zircon grains show luminous or dark grey cores in CL images that exhibit oscillatory zoning (**Figure 2**). The examined zircon grains are overgrown by dark grey rims which in some cases show euhedral shape. A dominant age peak is observed in the sample at 1845 Ma with two subordinates at 1320 Ma and 1656 Ma (**Figure 3**). The youngest detrital zircon grain of the sample yielded a concordia age of 1237 ± 8 Ma (2s) that is regarded as the maximum depositional age of the Barrois Complex. The selected zircon grains show Th/U values from 0.16 to 1.98 indicating magmatic origin of the selected grains.

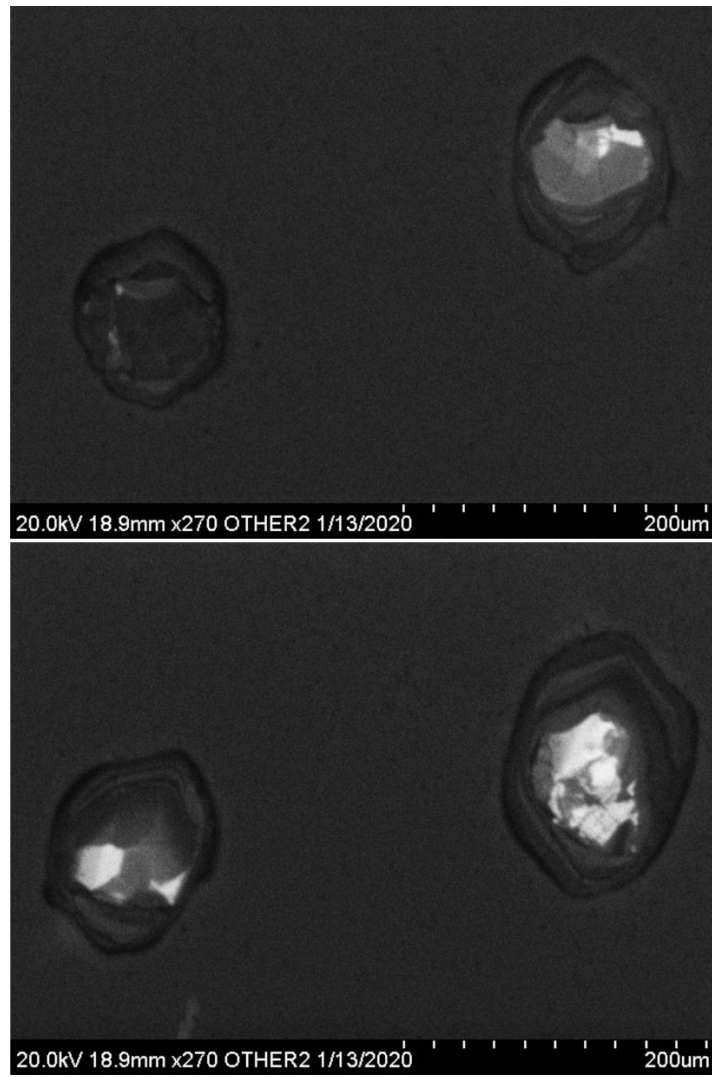


Figure 2. Representative cathodoluminescence images of zircon grains from the sample 2019-AM-0002B1

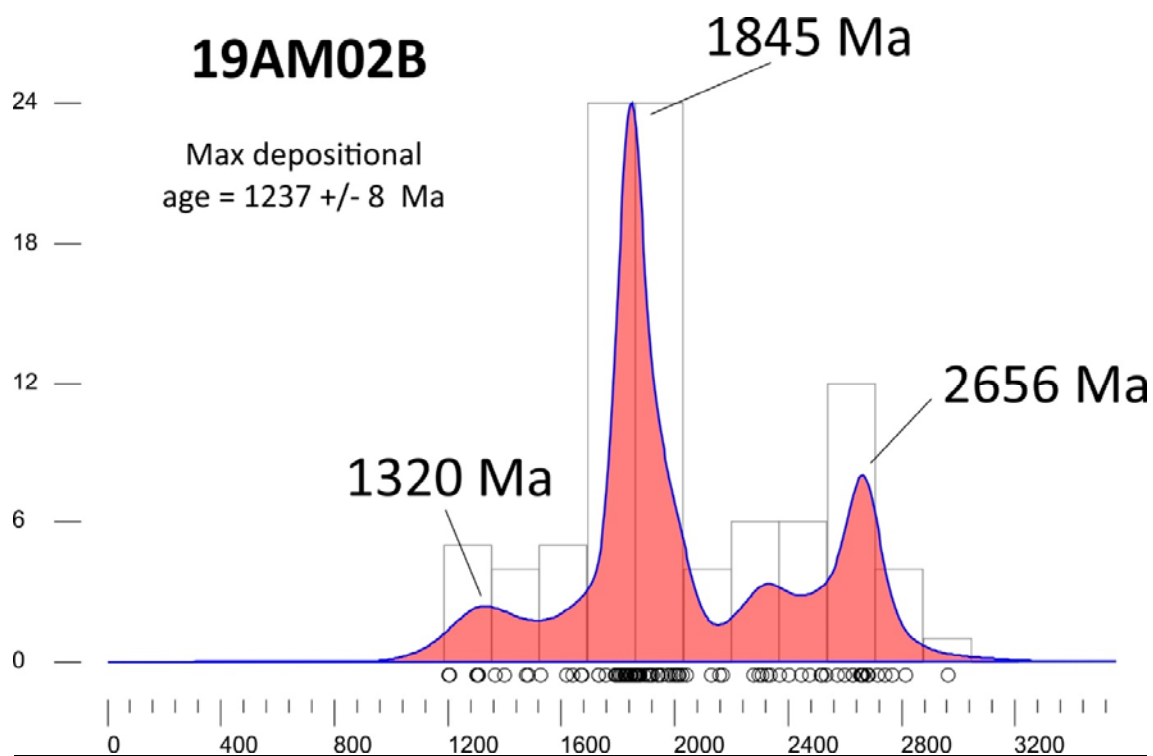


Figure 3. Kernel density estimation diagram of the sample 2019-AM-0002B1

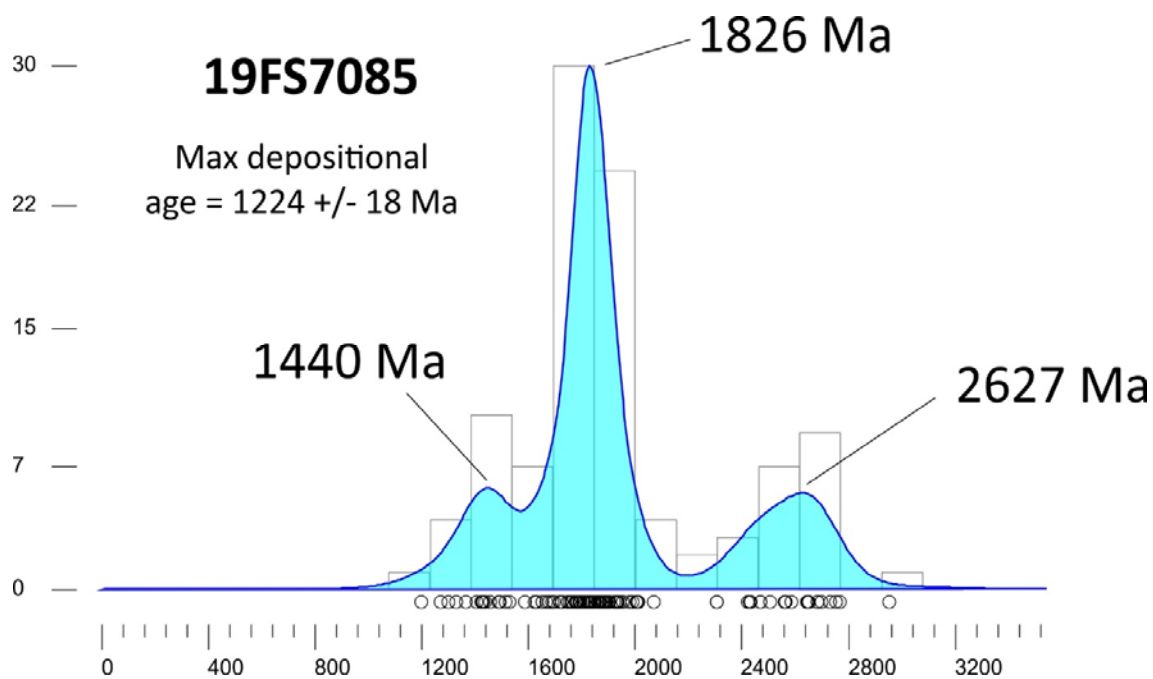


Figure 4. KDE plot of Pb-Pb ages and maximum depositional age from zircon grains of the sample 2019-FS-7085D1

Sample 2019-FS-7085D1 (Quartzite)

Zircon grains from the quartzitic sample 2019-FS-7085D1 exhibit bright and dark, oscillatory and sector-zoned cores overgrown by two or three generations of mantle and rim domains (**Figure 5**). The selected grains show variable external morphologies from subhedral to rounded recording variable degrees of abrasion and transport distance. The analyses were located onto core and rim domains of the selected grains and were filtered for discordance (cut-off value = 10%) and Th/U values (Th/U <0.1) to avoid analyses from metamorphic domains that were grown in-situ. In total, one-hundred-two analyses (n=102) were kept after filtering, yielding three major $^{207}\text{Pb}/^{206}\text{Pb}$ age peaks at 1.82 Ga, 2.6 Ga, and 1.42 Ga (**Figure 4**) with the youngest concordia age yielding an age of 1224 ± 18 Ma indicating possibly similar depositional setting and sources with Wabash-type quartzite bodies in the wider area.

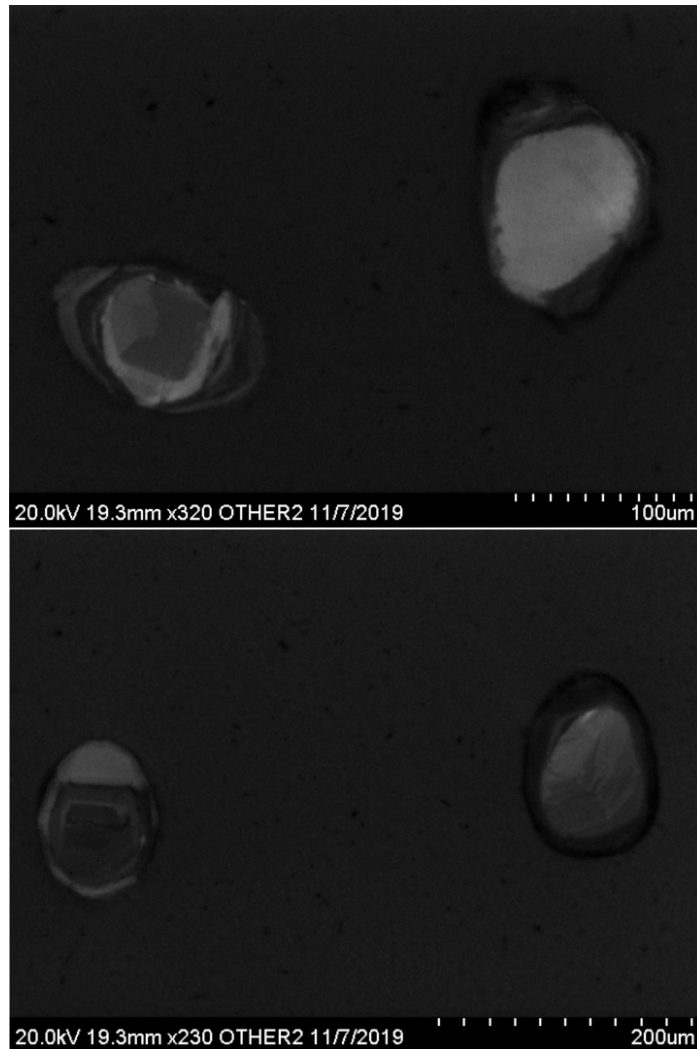


Figure 5. Representative CL images of zircon grains from the sample 2019-FS-7085D1

Sample 2019-AM-0167A1 (Granite)

The zircon grains of the sample 2019-AM-0167A1 are subhedral and show bright cores in CL images, occasionally with oscillatory zoning, overgrown by darker rims (**Figure 8**). The U concentration of the examined grains varies from 66.9 to 1638 ppm with an average value of 361 ppm. The U-Pb isotopic analyses of core domains with Th/U values above 0.1 yield an upper intercept U-Pb date of 1364 ± 9 Ma (**Figure 7**, 2σ , $n = 43$, $MSWD = 0.67$) that is interpreted as the crystallization age of the Opx-bearing syenite. Zircon domains with dark response in CL images and Th/U values < 0.1 yield an upper intercept date of 1090 ± 41 Ma (**Figure 9**, 2σ , $n = 4$, $MSWD = 0.3$) that is interpreted as the age of metamorphic zircon growth.

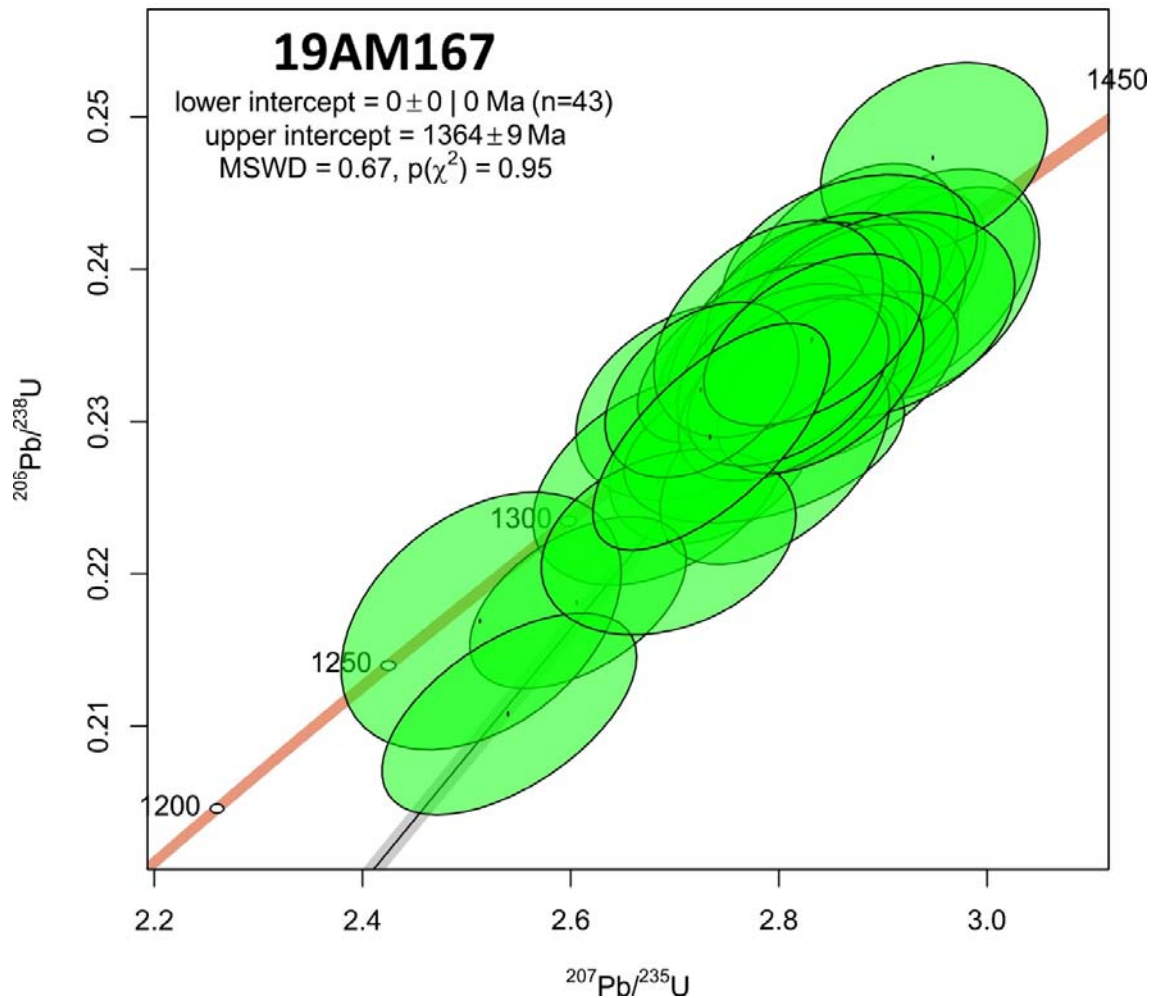


Figure 7. U-Pb concordia diagram of zircon cores from the sample 2019-AM-0167A1

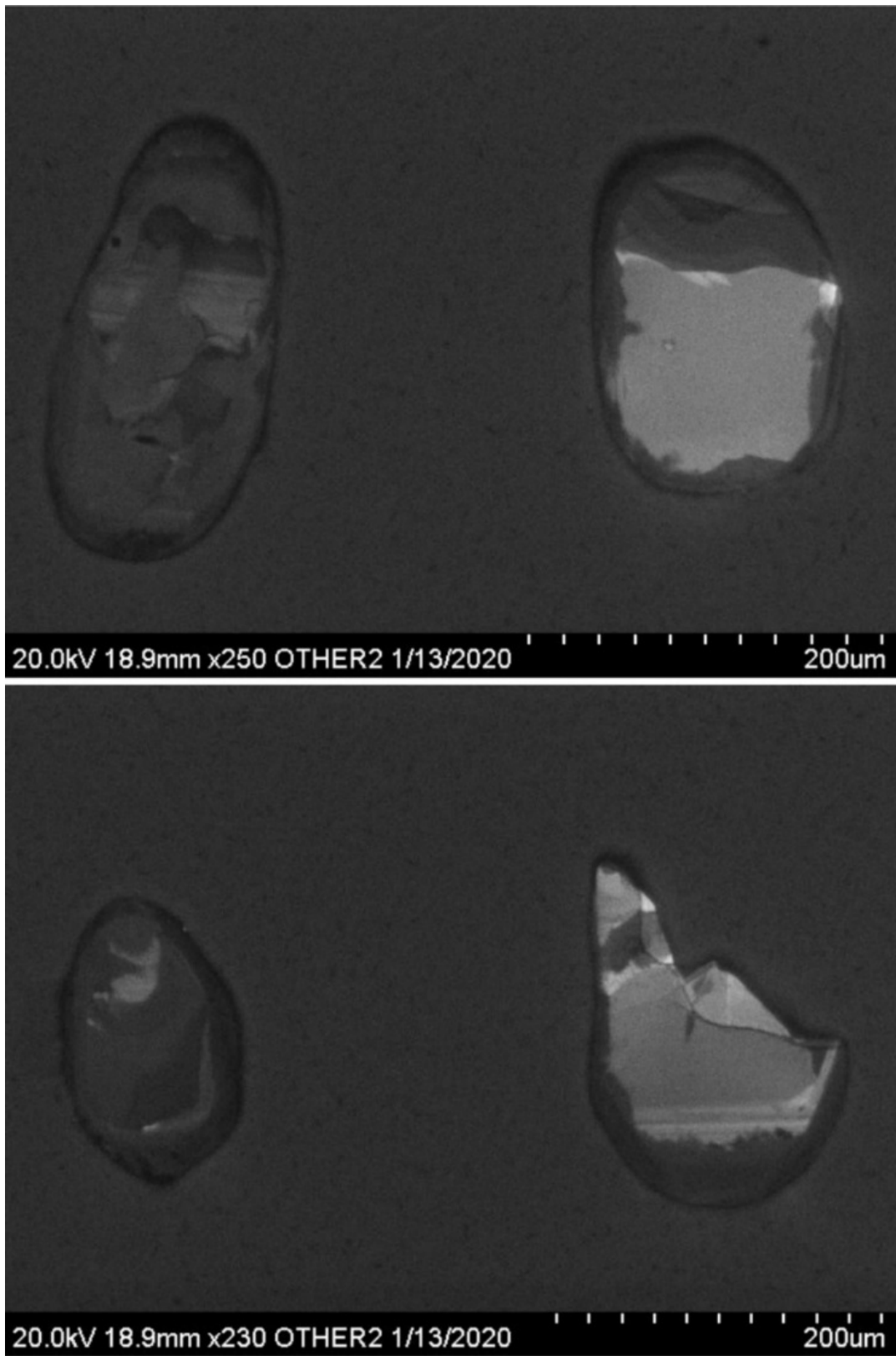


Figure 8. Representative CL images of zircon grains from the sample 2019-AM-0167A1

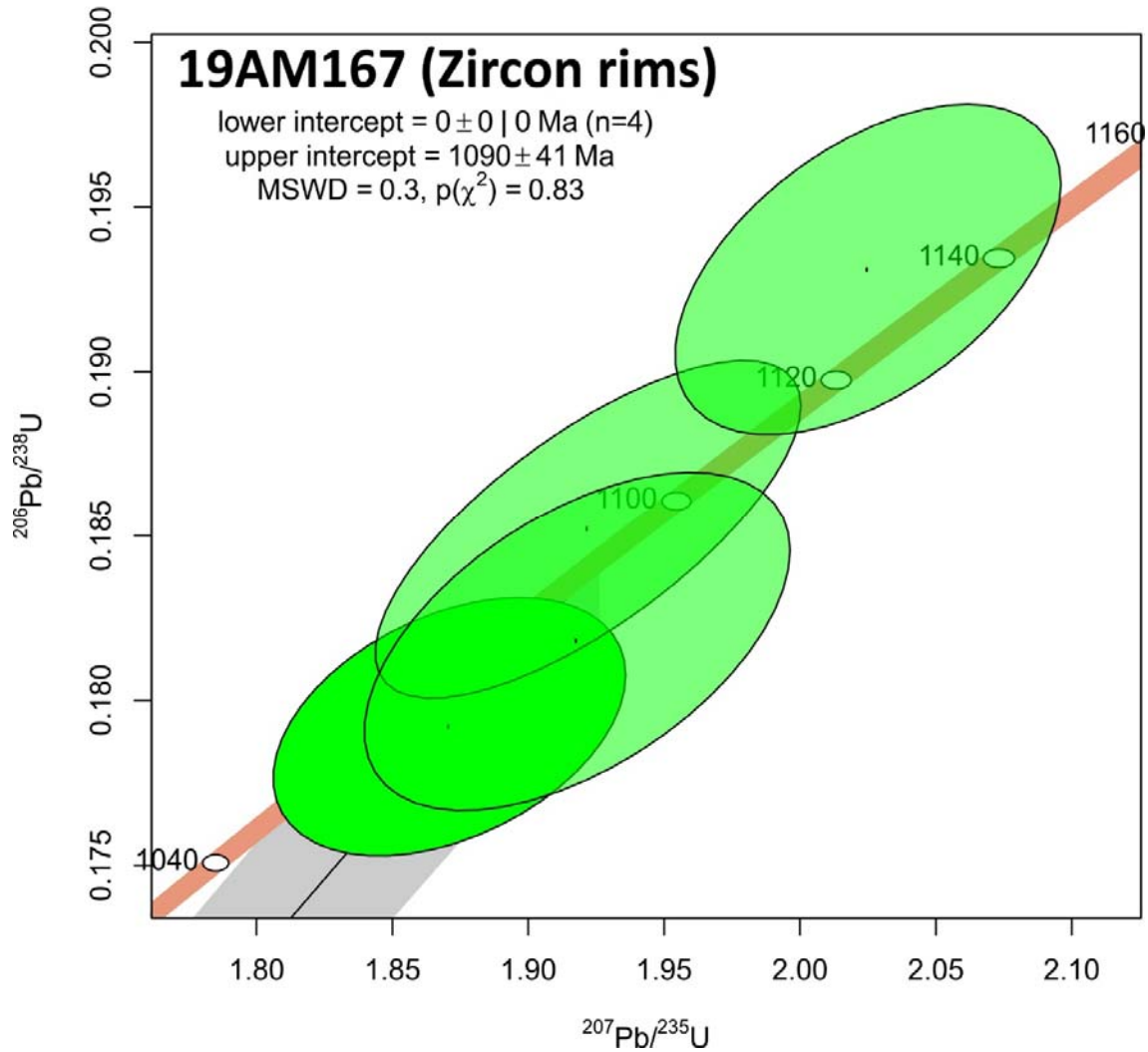


Figure 9. U-Pb concordia diagram of zircon rims from the sample 2019-AM-0167A1

Sample 2019-AM-0170A1 (Mangerite)

The zircon grains show subhedral morphology and aspect ratios 2:1 to 4:1. In CL images the examined grains show luminous cores, commonly with oscillatory zoning, but grains with homogeneous grey response in CL are also common (**Figure 10**). The U concentration of the examined grains varies from 47 to 644 ppm with an average value of 150 ppm. The U-Pb isotopic analysis of intragrain domains with Th/U > 0.1 yielded an upper intercept U-Pb date of 1021 ± 15 Ma (**Figure 11**, 2σ , n = 42, MSWD = 0.97) that is interpreted as the magmatic crystallization age of the mangerite.

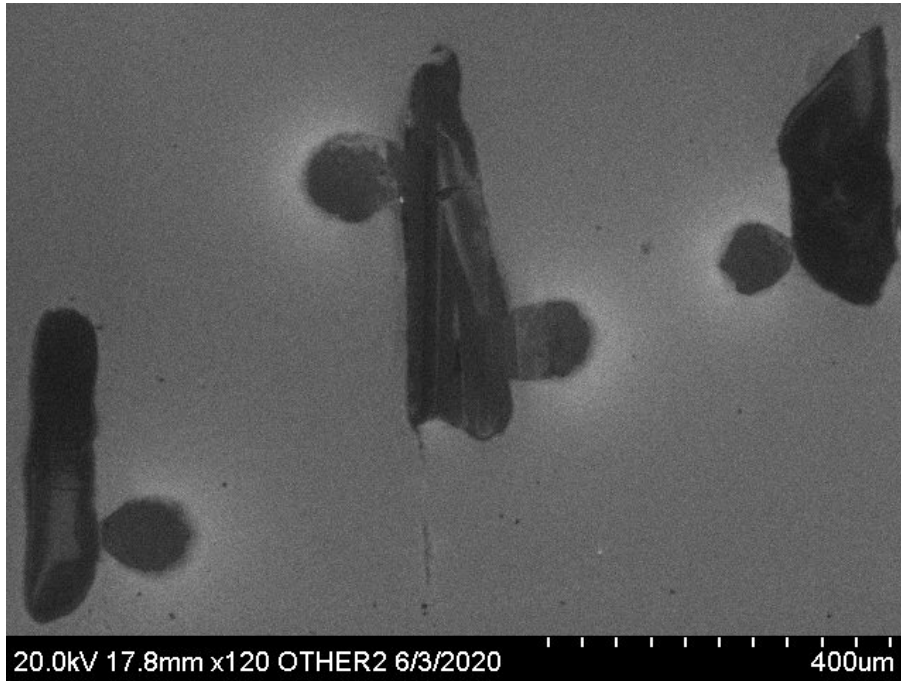


Figure 10. Representative CL images of zircon grains from the sample 2019-AM-0170A1

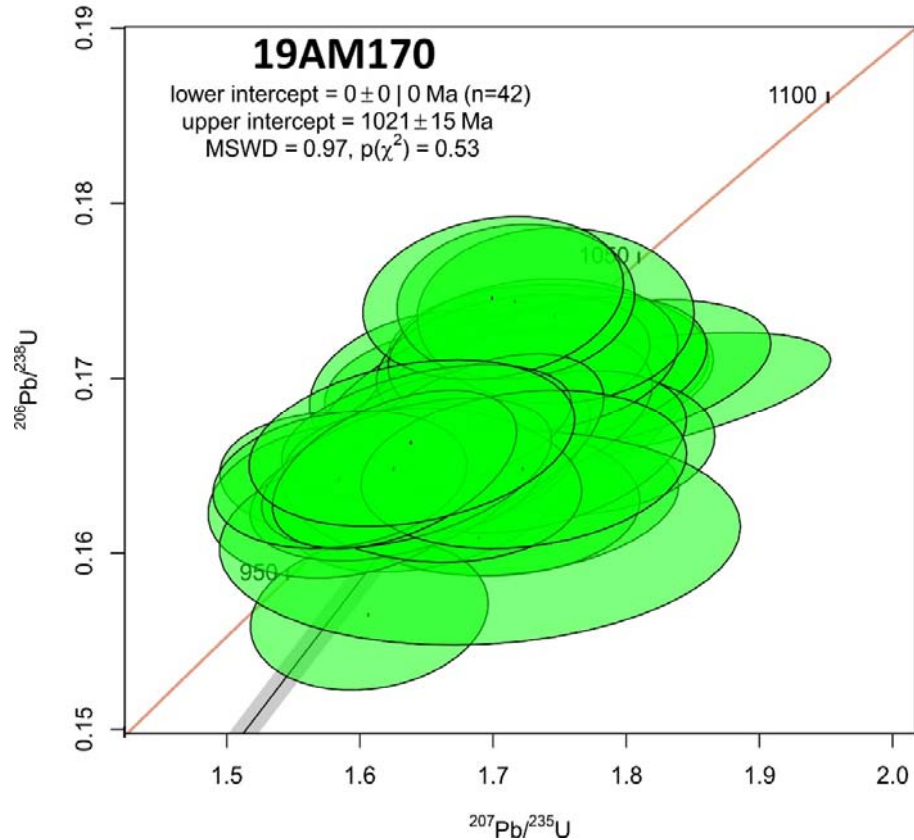


Figure 11. U-Pb concordia diagram of the sample 2019-AM-0170A1

Sample 2019-AB-5002A1 (Mangerite)

The examined zircon grains of the mangerite 2019-AB-5002A1 are anhedral with aspect ratios 1:1 to 3:1. The grains show homogeneous luminous cores in CL, occasionally with oscillatory zoning, overgrown by dark grey in CL domains (**Figure 13**). The U concentration of the examined grains varies from 41.2 to 435 ppm with an average value 136 ppm. Zircon grains that show homogeneous grey response in CL are also common. The U-Pb isotopic analysis of zircon grains with Th/U values > 0.1 yielded an upper intercept U-Pb age of 1015 ± 13 Ma (**Figure 12**, 2σ , $n = 41$, MSWD = 0.54) that is interpreted as the magmatic crystallization age of the mangerite.

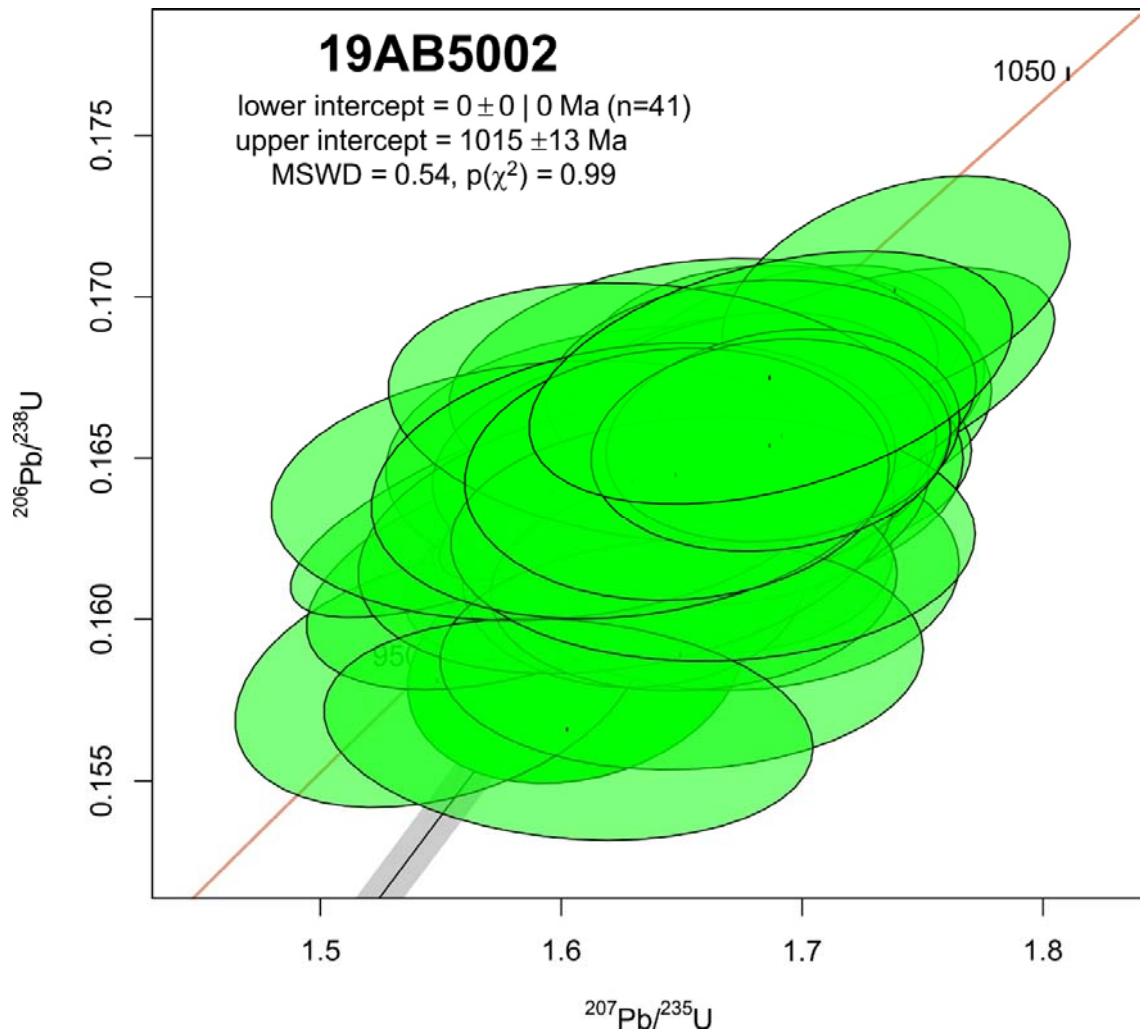


Figure 12. U-Pb concordia diagram of the sample 2019-AB-5002A1

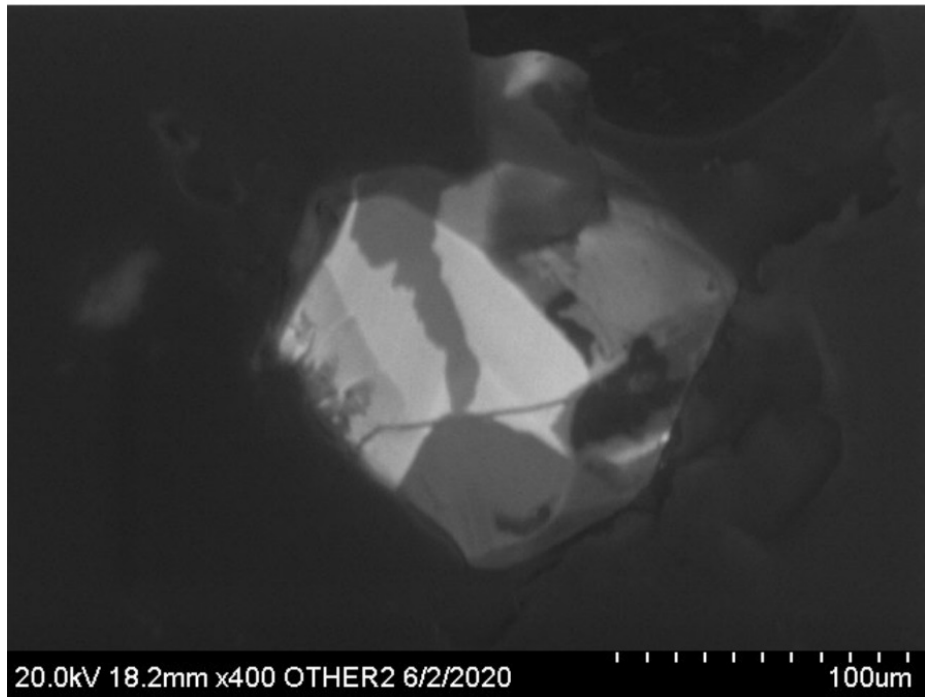
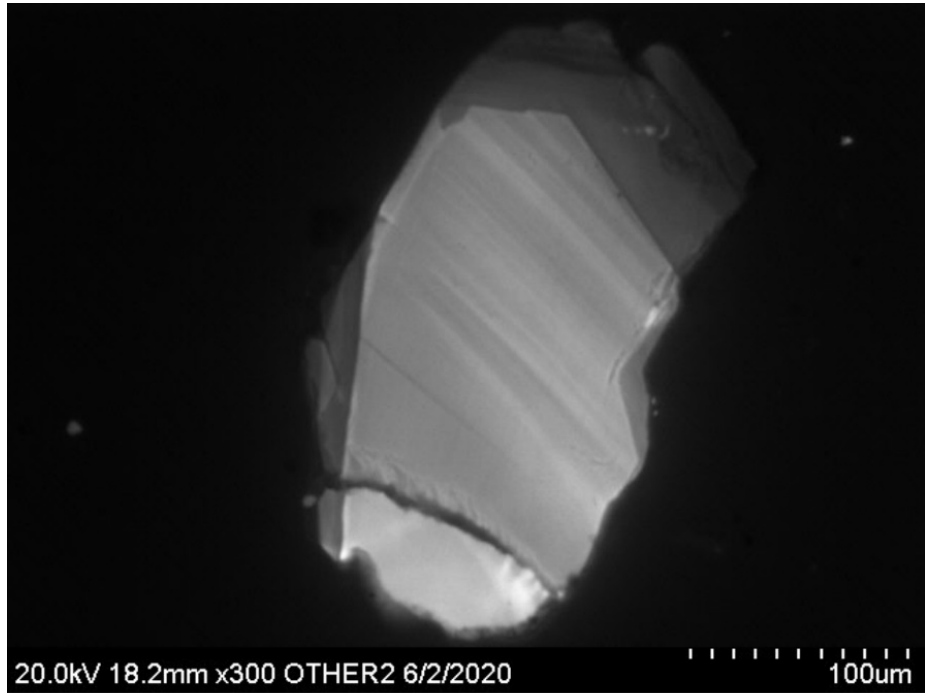


Figure 13. Representative CL images of zircon grains from the sample 2019-AB-5002A1.

Sample 2019-AM-0067A1 (Mangerite)

The examined zircon grains show luminous cores in CL images, occasionally with oscillatory zoning, overgrown by sub to euhedral dark grey domains in CL images (**Figure 15**). The U concentration of the examined grains varies from 21.1 to 415 ppm with an average value of 102 ppm. The U-Pb isotopic analysis of the luminous in CL domains with Th/U > 0.1 yielded an upper intercept U-Pb age of 1031 ± 17 Ma (**Figure 14**, 2σ , $n = 54$, MSWD = 1.4) that is interpreted as the age of magmatic crystallization of the mangerite.

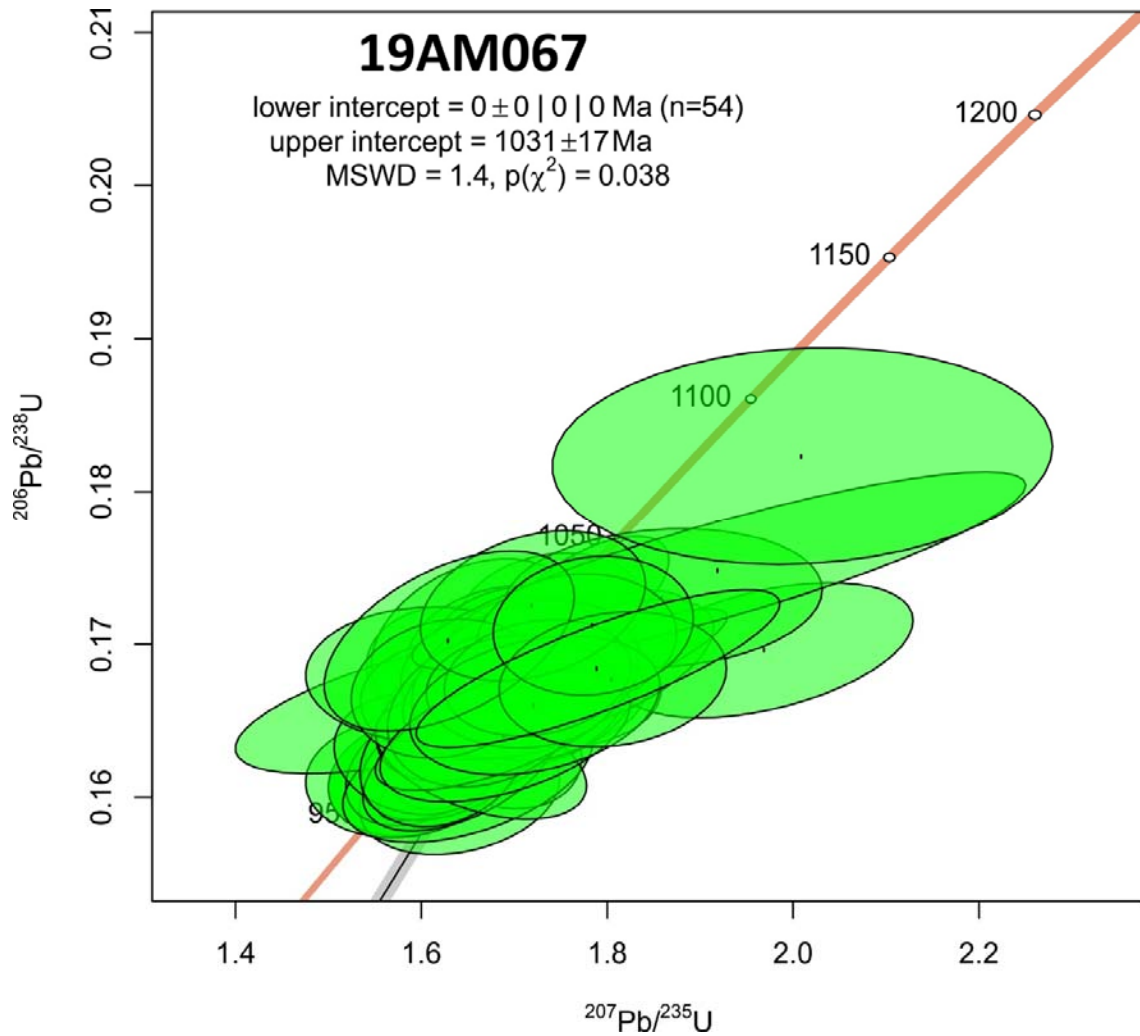


Figure 14. U-Pb concordia diagram from zircon grains of the sample 2019-AM-0067A1

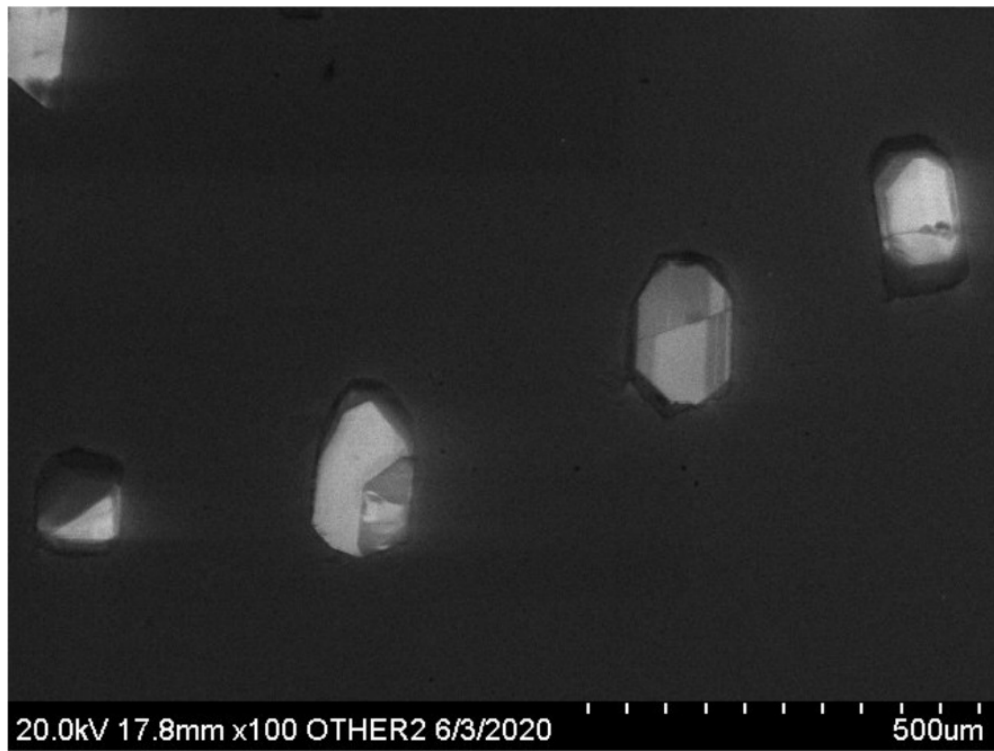
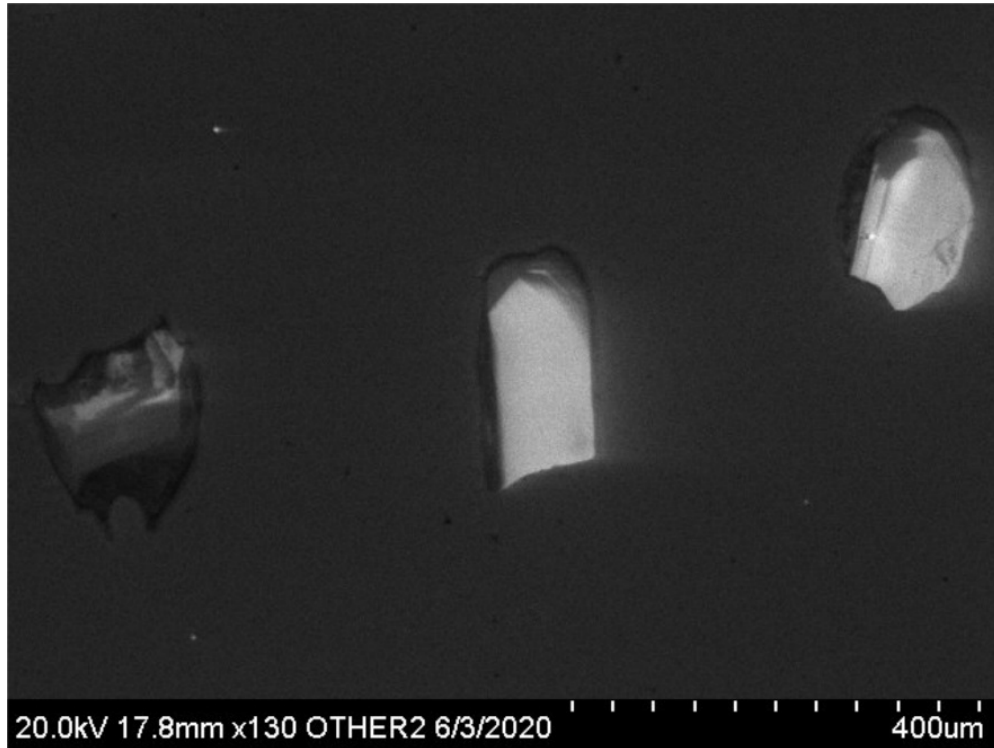


Figure 15. Representative CL images of zircon grains from sample 2019-AM-0067A1.

Sample 2019-AM-0187A1 (Mangerite)

The examined zircon grains are subhedral to anhedral with aspect ratios 1:1 to 4:1. In CL images they exhibit commonly bright cores either homogeneous or with faint oscillatory zoning (**Figure 16**). Grey to dark grey in CL homogeneous core domains are also common. The U contents of the examined grains varies from 75 to 452 ppm with an average value of 213 ppm. The U-Pb isotopic analysis of the core domains yielded an upper intercept U-Pb age of 1039 ± 15 Ma (**Figure 17**, 2σ , $n = 37$, MSWD = 1.3) that is interpreted as the magmatic crystallization age of the mangerite.

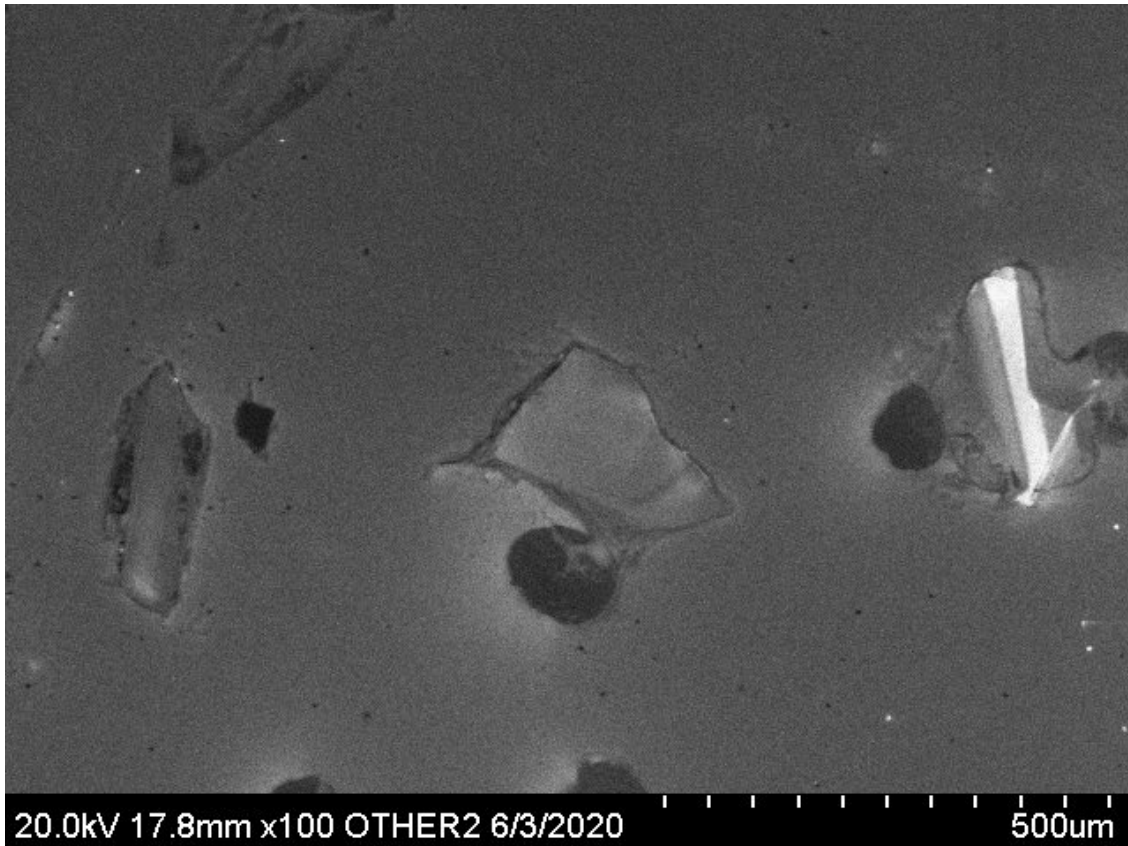


Figure 16. Representative CL images of zircon grains from the sample 2019-AM-0187A1.

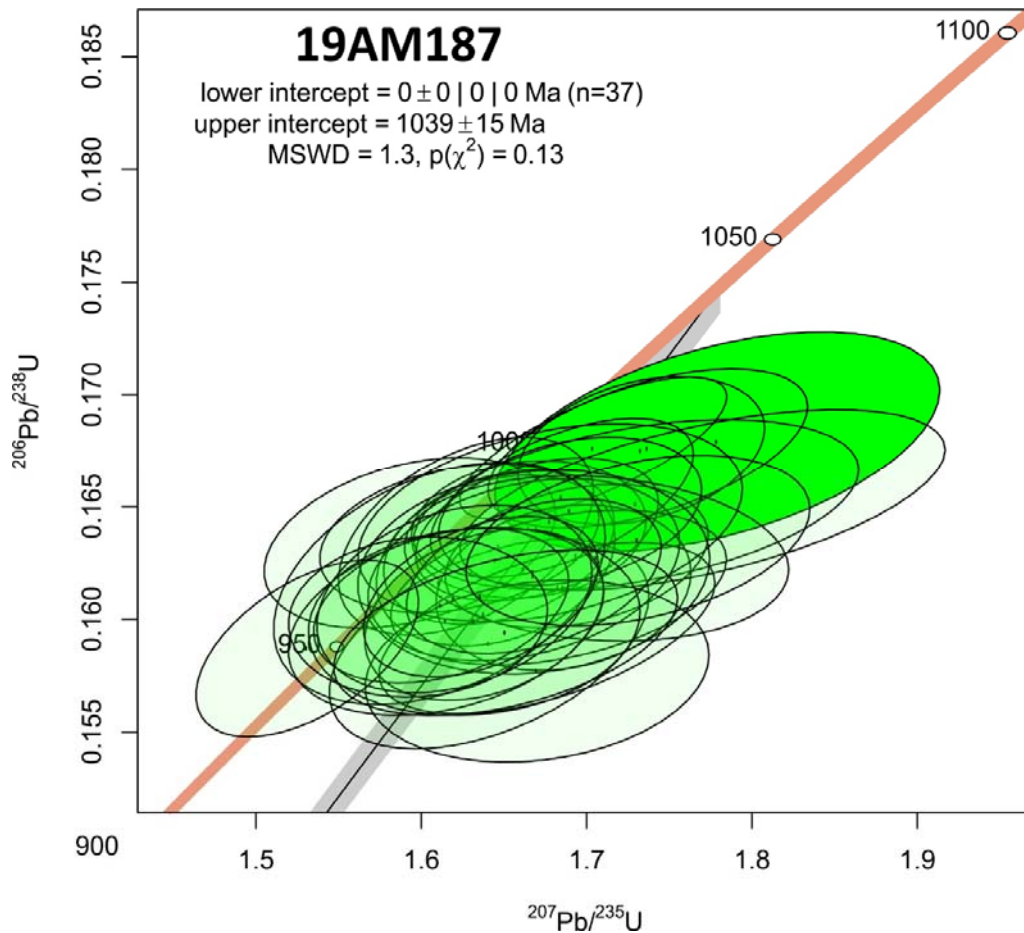


Figure 17. U-Pb concordia diagram of the sample 2019-AM-0187A1.

Sample 2019-AM-0186A1 (Alkali feldspar-bearing granite)

The zircon grains of the sample are euhedral to subhedral with aspect ratios 2:1 to 4: 1. The grains in the CL images show luminous cores, commonly with oscillatory zoning, overgrown by darker in CL oscillatory-zoned mantle domains and dark rims of possible metamorphic origin. The examined grains show U contents from 23 to 614 ppm with an average value of 155 ppm and Th/U ratios varying from 0.51 to 1.73 indicating magmatic origin of the targeted intragrain domains. The U-Pb isotopic microanalysis yielded an upper intercept age of 1042 ± 12 Ma (**Figure 18**, 2σ , $n = 54$, MSWD = 1.3) that is interpreted as the crystallization age of the alkali feldspar-bearing granite (**Figure 19**).

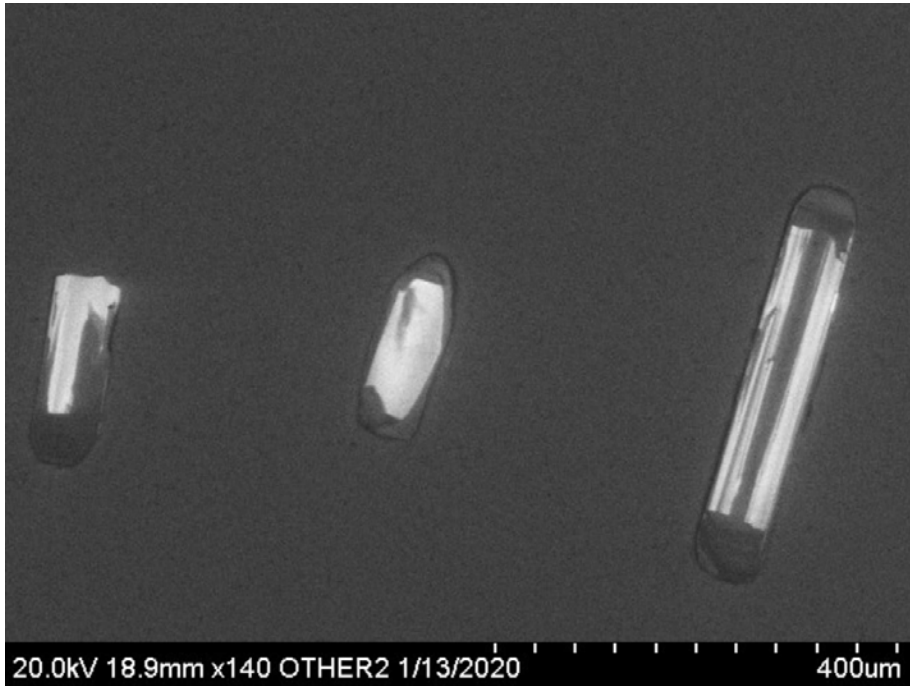


Figure 18. Representative CL images of zircon grains from sample 2019-AM-0186A1.

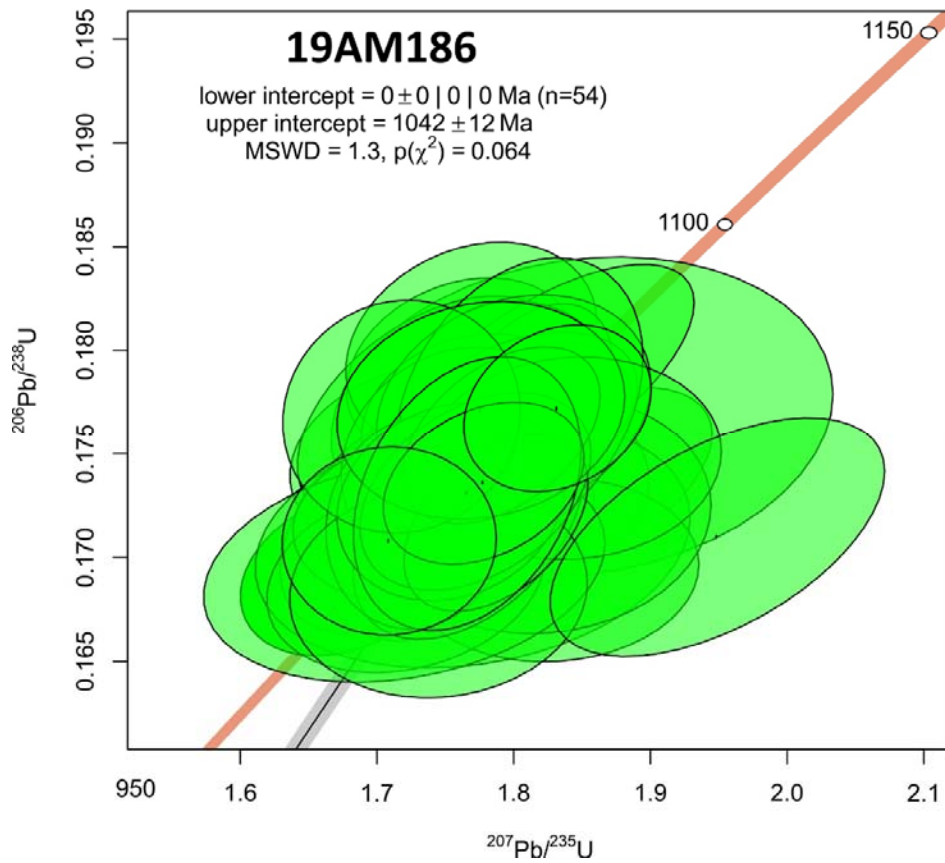


Figure 19. U-Pb concordia diagram of sample 2019-AM-0186A1.

Optical micrographs

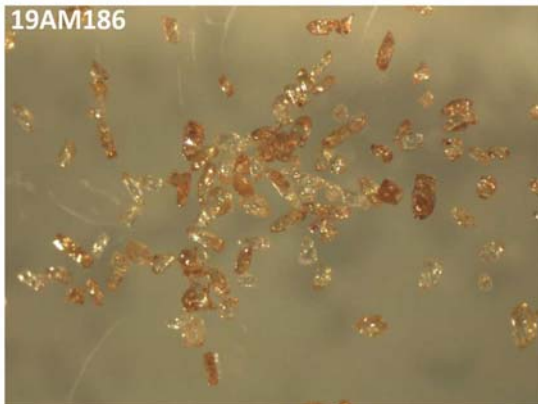
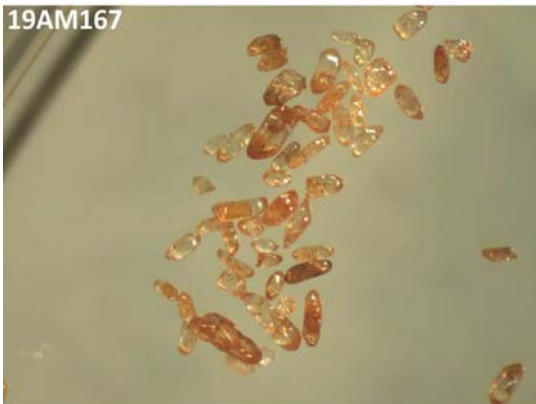
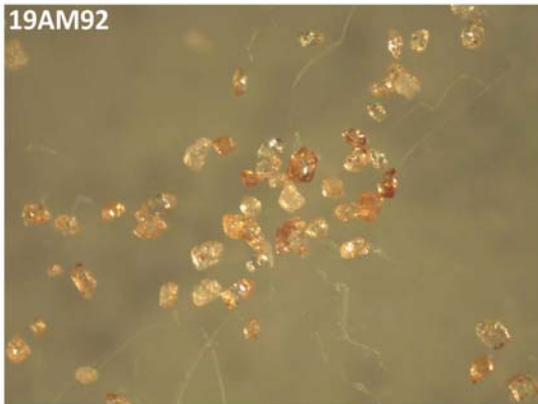
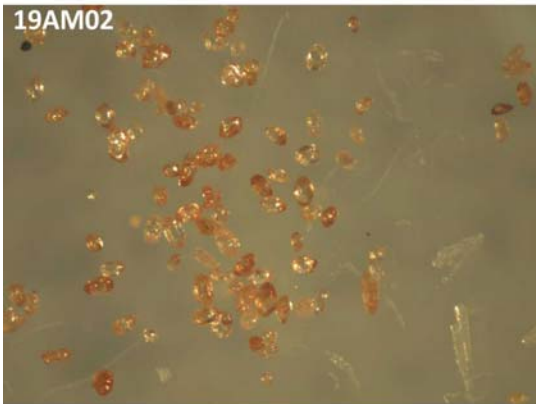
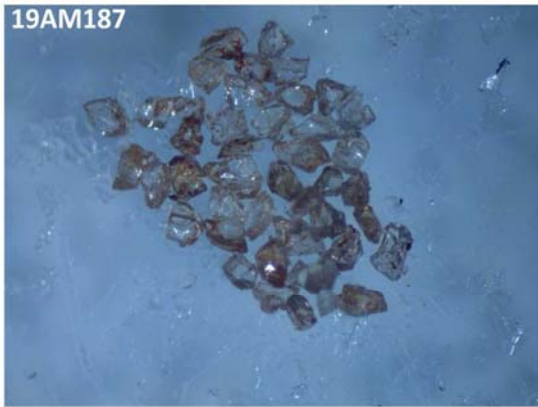
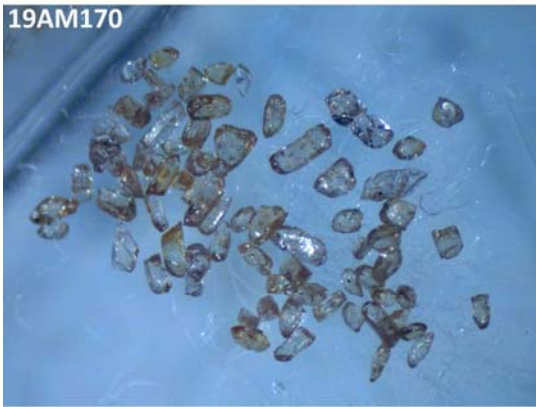


Figure 1. Optical micrographs of zircon grains from selected samples (FOV = 1mm)

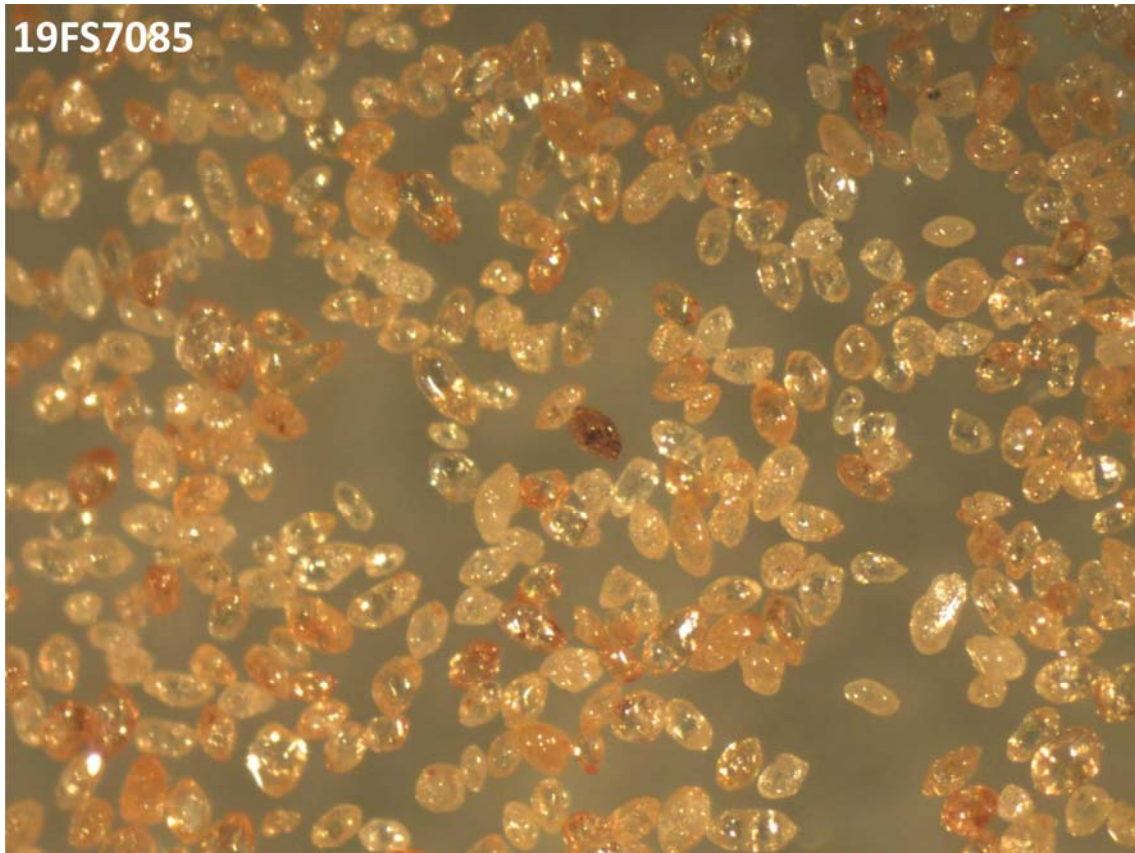


Figure 2. Optical micrograph of representative zircon grains from the sample 20190FS-7085D1 (FOV = 1 mm)

References

Higgins, M. D., & Van Breemen, O. (1996). Three generations of anorthosite-mangerite-charnockite-granite (AMCG) magmatism, contact metamorphism and tectonism in the Saguenay-Lac-Saint-Jean region of the Grenville Province, Canada. *Precambrian Research*. [https://doi.org/10.1016/0301-9268\(95\)00102-6](https://doi.org/10.1016/0301-9268(95)00102-6)

Van Breemen, O. (2009). Report on U-Pb geochronology for the Pimpuacan reservoir region. GSC contribution number 20080416

Vermeesch, P. (2018). IsoplotR: A free and open toolbox for geochronology. *Geoscience Frontiers*. <https://doi.org/10.1016/j.gsf.2018.04.001>